In-situ polymerization behaviour of bone cements

A. MAFFEZZOLI*, D. RONCA, G. GUIDA‡, I. POCHINI and L. NICOLAIS§
*Department of Materials Science, University of Lecce, Via per Arnesano, 73100, Lecce, Italy
‡Istituto di Clinica Ortopedica, Faculty of Medicine and Surgery, II University of Naples, Italy
§Department of Materials and Production Engineering, University of Naples ''Federico II'', Italy

The polymerization behaviour of bone cements during total hip replacements is characterized by a fast and highly non-isothermal bulk reaction. In the first part of this paper the reaction kinetics are analysed by calorimetric analysis in order to determine the rates of polymerization in isothermal and non-isothermal conditions. A phenomenological kinetic model, accounting for the effects of autoacceleration and vitrification, is presented. This model, integrated with an energy balance, is capable of predicting the temperature across the prosthesis, the cement and the bone and the degree of reaction in the cement, during *in situ* polymerization. The temperature and the degree of reaction profiles are calculated, as a function of the setting time, taking into account the system geometry, the thermal diffusivity of bone, prosthesis and cement, and the heat rate generated by the reaction according to the kinetic model. Material properties, boundary and initial conditions are the input data of the heat transfer model. Kinetic and heat transfer models are coupled and a numerical solution method is used. The model is applied in order to study the effects of different application procedures on temperature and degree of reaction profiles across the bone–cement–prosthesis system.

1. Introduction

The polymerization conditions of methyl methacrylate (MMA)-based bone cements significantly affect their properties and performances. During chain polymerization of MMA a series of complex independent reactions occurs, involving free radicals, monomers and long chain molecules [1]. Furthermore, during the polymerization of bone cements, dramatic rheological changes of the materials, involving the transformation of the viscous cement into a solid glass (vitrification), occurs. The growth of the polymeric chains is due to a monomer addition reaction that follows a first-order kinetic until a critical viscosity of the reactive mixture, corresponding to a given value of the degree of reaction, is attained. This point marks the onset of the so-called gel effect [1–7] during which a sudden increase of the reaction rate is observed. The effect of diffusion during polymerization is also responsible for the reaction end [4, 8–10] when the glass transition temperature, continuously increasing during polymerization, approaches isothermal polymerization causing a transition of the growing polymer in the glassy state (vitrification). In these conditions, the molecular mobility is strongly reduced and the reaction becomes diffusion controlled. Therefore, vitrification is responsible for a termination step in polymerization governed by this strong reduction in the molecular mobility before all the monomer is consumed.

During application of bone cement in total hip replacement, the bone and the prosthesis act as the boundaries of a true batch chemical reactor. As a consequence of the significant development of heat due to the exothermic nature of the polymerization reaction, a fast and highly non-isothermal bulk polymerization occurs. In particular, the cement/bone interface may be considered as a weak point, often responsible for the failure of total joint replacements [11, 12]. Improvements of the strength of this interface may be obtained, not only with good osseous penetration of the cement but also avoiding the tissue necrosis that may originate either from thermal or from chemical causes. The thermal effects of the polymerization are reflected in a significant peak temperature ranging between 80 °C and 124 °C in the cements [13] and between 48 °C and 105 °C at the bone/cement interface [14]. Poly methyl methacrylate (PMMA) and/or other fillers are usually added in order to reduce the heat evolved per unit mass of cement, and also if the filler weight fraction is limited by the viscosity of the cement. However, the peak temperature cannot be considered an exhaustive parameter for the determination of thermal damage to tissues. The time during which the tissues are exposed to a temperature higher than a threshold value must also be taken into account. As reported by Brauer *et al.* [14], between 48 °C and 60 °C, cell necrosis may occur depending on the exposure time, which at 50 °C ranges between 30 s and 400 s.

0957–4530

Toxic chemicals may arise from incomplete polymerization occurring in normal operative conditions determining high levels of unreacted monomer in the cement. The residual MMA, slowly released from the cement, may be responsible for tissue damage. The maximum degree of advancement of the polymerization reaction represents a measure of the amount of residual monomer in the bone cement.

A quantitative correlation between the temperature profiles and the degree of reaction across the bone–cement–prosthesis system and the polymerization conditions is not available in the literature. The final properties of the cement are significantly dependent on process variables, such as the mixing procedure and temperature and the geometry of the prosthesis and of the cavity. Accurate control of these variables may be considered a necessary step in order to obtain constant properties for the same cement used by different surgeons, and in order to perform laboratory tests that are representative of *in situ* polymerization conditions. Only optimization of the processing parameters in surgical practice can lead to the definition of the true limits of the existing cements. Improvement in biocompatibility or mechanical or processing characteristics of existing cements may not be achieved without considering the correlation among properties structure and processing. In particular, polymerization kinetics play a fundamental role in the determination of temperature and degree of reaction profiles during application.

In this paper, the isothermal and non-isothermal polymerization behaviour of a commercial bone cement is described. In the first part the reaction kinetic is analysed by differential scanning calorimetry (DSC). DSC data are used for the quantitative determination of the rates of polymerization in isothermal and non-isothermal conditions. A phenomenological kinetic model, already applied to thermosetting systems, is presented. The experimental DSC data are processed to calculate the parameters of the kinetic model.

This model is integrated with an energy balance in order to predict the temperature across the prosthesis, the cement and the bone, and the degree of reaction in the cement during non-isothermal polymerization. Temperature and degree of reaction profiles are calculated as a function of the setting time, taking into account the system geometry, the thermal diffusivity of bone, prosthesis and cement, and the heat rate generated by the polymerization reaction according to the kinetic model. Material properties, boundary and initial conditions and kinetic behaviour are the input data of the heat transfer model. Kinetic and heat transfer models are coupled and a numerical solution method is used. The model is applied to the study of the effects of different thicknesses and initial temperature of the cement on temperature and degree of reaction profiles across the bone–cement–prosthesis system.

2. Experimental procedure

A commercial radiopaque bone cement, Surgical Simplex P, kindly supplied by Howmedica, was analysed. The powder and liquid monomer, whose composition is reported in Table I, were mixed according to the instructions of the supplier (1/3 by volume of monomer and 2/3 by weight of powder).

TABLE I Composition of the material studied

Powder	Composition by weight (%)
Polymethyl methacrylate	15
Methyl methacrylate-styrene copolymer	75
Barium sulphate U.S.P.	10
Unknown initiator (probably benzoyle peroxide)	?
Liquid monomer	**Composition by volume (%)**
Methyl methacrylate	97.4
N,N-dimethyl para toluidine	2.6
Hydroquinone	75 ± 15 ppm

Calorimetric analysis was carried out with a differential scanning calorimeter (DSC), Mettler DSC 30, operating with constant nitrogen flow of 100 cm^3/min. Sample preparation (6–10 mg) was performed at 20 °C using a constant mixing time of 1.5 min. The overall time, from contact of the monomer with the powder (i.e. with the initiator) to the beginning of the DSC test was 2.5 min. The samples, weighed after each experiment, showed negligible evaporation of monomer (less than 0.2 mg).

3. Polymerization kinetics

3.1. General behaviour

A typical DSC thermogram obtained at 30 °C is reported in Fig. 1. The delay in the DSC signal represents an induction time, a relevant parameter from a processing point of view, associated with the reaction between initiator and inhibitor (hydroquinone) [8]. Hydroquinone is present in the cement in order to prevent incipient polymerization during storage and to delay the onset of polymerization reaction for the time required for the insertion of the cement and positioning of the prosthesis. However, only a small amount of hydroquinone may be added as a consequence of its toxicity [14]. The induction time (t_i) (Fig. 1), which may be considered as the only detectable macroscopic parameter representative of the inhibitor–initiator reaction, shows the following temperature dependence:

$$t_i = 1/[K_{to} \exp(-E_t/RT)] \quad (1)$$

The induction times, measured in different isothermal DSC experiments and corrected for the sample preparation time, are used to compute the parameters of Equation 1 by linear regression (Table II). Good agreement between experimental data and model results is observed in Fig. 2.

DSC measurements may be used for determination of the advancement of polymerization by assuming that the heat evolved during the polymerization reaction is proportional to the overall extent of the

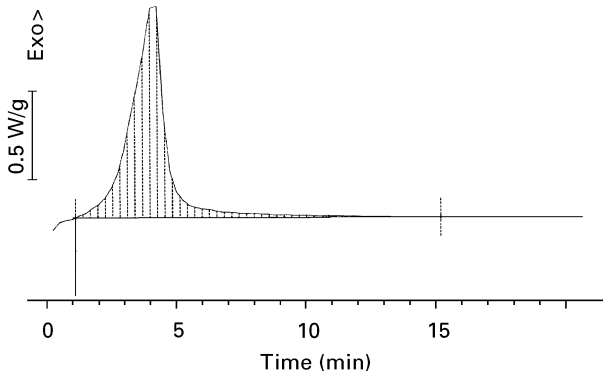

Figure 1 Isothermal DSC thermogram obtained during polymerization at 30 °C.

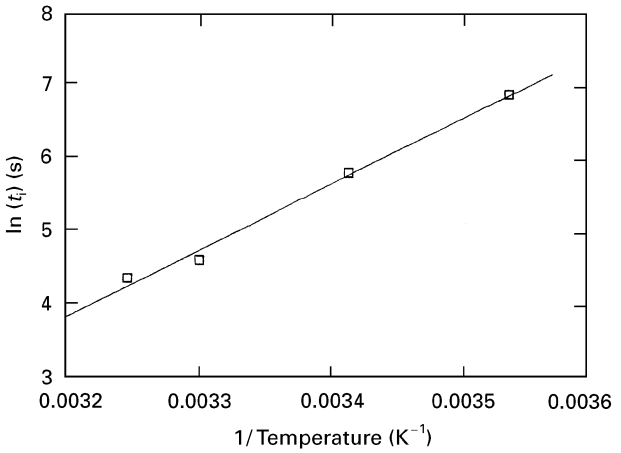

Figure 2 Temperature dependence of the isothermal induction times.

reaction, given by the fraction of reactive groups consumed. Following this approach the degree of reaction, α, is defined as:

$$\alpha = Q(t)/Q_{tot} \quad (2)$$

where $Q(t)$ is the partial heat of reaction developed during a DSC experiment and Q_{tot} represents the maximum heat of reaction measured in a non-isothermal experiment, taken as a reference value. The reaction rate, $d\alpha/dt$, is thus obtained from the heat flow dQ/dt as:

$$d\alpha/dt = 1/Q_{tot}(dQ/dt) \quad (3)$$

A value of $Q_{tot} = 125$ J/g is assumed as an average of the heats of reaction measured in non-isothermal experiments. It must be noted that this value, if referred to the weight of MMA, is lower (375 J/g) than the theoretical heat of polymerization of MMA (550 J/g). This can be explained assuming that the liquid monomer is an oligomer rather than pure MMA, or that limited increase of the average molecular weight during storage has occurred.

The heat developed during isothermal DSC experiments (Q_{is}) is lower than Q_{tot}, indicating that unreacted monomer is still present. Then a maximum degree of reaction, α_m, may be introduced:

$$\alpha_m = Q_{is}/Q_{tot} \quad (4)$$

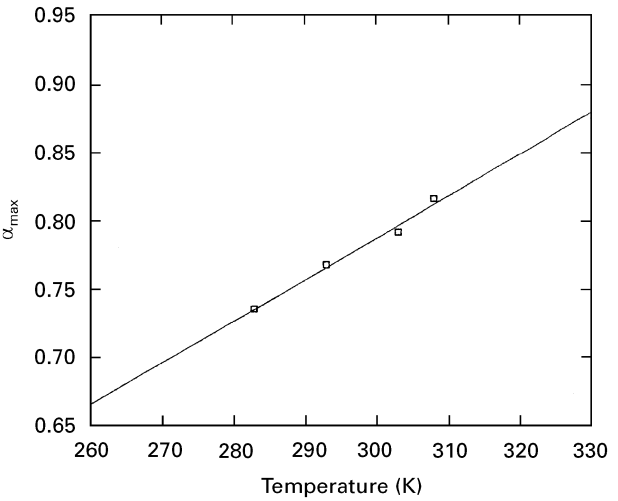

Figure 3 Temperature dependence of the maximum degree of reaction obtained from isothermal DSC polymerization experiments.

TABLE II Parameters of the kinetic model

Parameter	Value	Parameter	Value
n	0.7	a	− 0.1336
m	0.86	$b(K^{-1})$	0.00307
$\ln(K_o)(s^{-1})$	18.8	$\ln(K_{to})(s)$	− 25.71
$E_a/R(K)$	6600	$E_t/R(K)$	9223

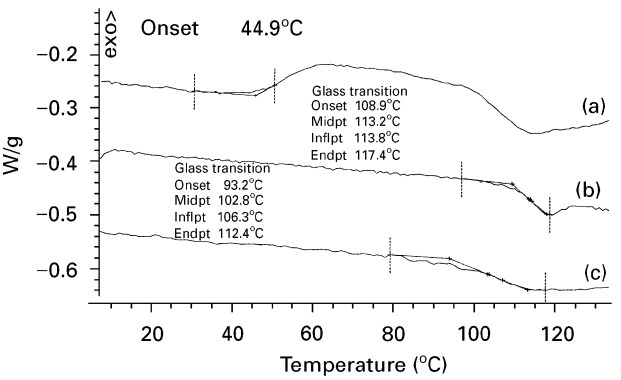

Figure 4 DSC thermograms obtained at 10 °C/min on a sample previously cured at 30 °C (trace (a)), on the powder sample (trace (b)) and on a fully cured cement sample (trace (c)) (traces (b) and (c) are vertically shifted).

The temperature dependence of α_m, shown in Fig. 3, can be well represented by a linear relationship [8–10]:

$$\alpha_m = a + bT \quad \text{for } T < T_{gmax};$$
$$\alpha_m = 1 \quad \text{for } T > T_{gmax} \quad (5)$$

When the temperature approaches the glass transition temperature (T_g) of the fully polymerized system (T_{gmax}), $\alpha_m = 1$. The fitting parameters a and b are reported in Table II. The presence of unreacted monomer may be revealed by heating a sample after isothermal polymerization. The thermogram of Fig. 4 (trace (a)) was obtained at 10 °C/min on a sample polymerized at 30 °C. A typical residual reactivity peak, located at a temperature of 10–15 °C higher than

the polymerization temperature, is observed, indicating that the material is not fully polymerized. As shown in Fig. 4 (trace (a)), the reaction may restart in conditions of enhanced molecular mobility by simply heating the sample at a temperature higher than the T_g developed during the former isothermal polymerization. Since the rate of reaction is very high compared with the structural volume relaxation occurring during the glass transition, vitrification is not able to instantaneously arrest the reaction, as observed for thermosetting resins [8–10, 15], and the T_g may reach a temperature of 10–15 °C higher than the polymerization temperature. For these reasons the onset of residual reactivity may be considered as a measure of the T_g of a blend of three components:

(1) the isothermally polymerised PMMA;
(2) the polymeric fraction of the powder;
(3) the unreacted monomer (MMA).

If vitrification occurs when the T_g of the blend PMMA/powder/MMA (T_{gb}) reaches the test temperature, the T_g of the growing PMMA could be calculated from the weight fraction (W_i) of the three components using the Fox equation [16]:

$$\frac{1}{T_{gb}} = \sum_{i=1}^{n} \frac{w_i}{T_{gi}} \tag{6}$$

The glass transition temperature of the powder ($T_{gp} = 386$ K) is calculated by the thermogram reported in trace (b) of Fig. 4. A T_g of the blend unreacted MMA/powder of 225 K is measured by DSC and, applying Equation 6, a glass transition temperature of MMA, $T_{gMMA} = 129$ K, is calculated. The T_g of PMMA (T_{gPMMA}) polymerized at 30 °C may be evaluated, with some approximation, from Equation 6 using T_{gb}, T_{gMMA} and T_{gp}. The onset of the residual reactivity peak reported in trace (a) of Fig. 4 is assumed to be the closest value of T_{gb} that can be measured. A $T_{gPMMA} = 385$ K, in accordance with the values (378–386 K) reported in the literature [17], is obtained. Although the calculated value of T_{gPMMA} is practically equal to that of the powder ($T_{gp} = 386$ K), the unreacted monomer still present, acting as a plasticizer, lowers the glass transition temperature of the cement experimentally observed by DSC to T_{gb}.

The thermogram obtained when heating at 10 °C/min a sample polymerized in non-isothermal conditions to 150 °C, is reported in Fig. 4 (trace (c)). In this case the residual reactivity peak is not detected, while a glass transition temperature of the cement $T_{gc} = 376$ K, 10 °C lower than the T_g of the powder, is clearly shown. This value represents the T_g of the blend of PMMA just polymerized and of the polymer fraction of the powder. T_{gc} is lower than T_{gp} probably because of the presence of unreacted MMA. It must be noted that, when applying Equation 6 to a blend of powder and MMA, a very small weight fraction of MMA (about 1%) lowers the T_{gp} by 10 K!

3.2. Kinetic modelling

The chain polymerization reactions, as mentioned above, are dominated by the effect of diffusion at the beginning (gel effect) and at the end of polymerization (vitrification). For this reason, the rather simple expression obtained at constant temperature in steady state conditions [1], accurately represents the kinetic behaviour only for low values of the degree of reaction ($\alpha < 0.2$):

$$\frac{d\alpha}{dt} = k_p \left(\frac{2fk_i}{k_t}\right)^{0.5} (1 - \alpha) \tag{7}$$

In Equation 7, k_p, k_i, and k_t represent the kinetic constants of propagation, initiation and termination reaction, and f the initiator efficiency. In particular, the gel effect occurs at lower values of the degree of reaction when a non-reactive polymer is added to the monomer [7]. For a reactive system containing a high fraction of non-reactive polymer, as in the case of bone cements, autoacceleration virtually occurs at the beginning of reaction.

Although many complex models have been reported in the literature for the polymerization of MMA [2–6], this shift of the onset of gel effect at the reaction start may lead to a simpler kinetic model. Since a decrease of k_t is responsible for the gel effect, and a decrease of k_p is responsible for termination when vitrification occurs, these constants may be considered dependent on the degree of reaction as follows:

$$k_t = k'_t \alpha^{-2m} \qquad k_p = k'_p (\alpha_m - \alpha)^n \tag{8}$$

Therefore the two diffusion effects that are responsible for the deviation of kinetic behaviour from Equation 7 may be taken into account using a simple pseudo-autocatalytic expression, obtained by modifying a kinetic equation previously proposed for unsaturated polyester and acrylic thermosetting resins [8, 20]:

$$d\alpha/dt = K \alpha^m (\alpha_m - \alpha)^n (1 - \alpha) \tag{9}$$

where m and n are fitting parameters not dependent on temperature and $K = k'_p (2fk_i/k'_t)^{0.5}$ is a single temperature-dependent rate constant given by an Arrhenius-type equation:

$$K = K_o \exp(-E_a/RT) \tag{10}$$

where K_o is the pre-exponential factor, R is the gas constant, E_a the activation energy and T the absolute temperature. The temperature dependence of α_m in Equation 9 is given by Equation 5.

The full model, given by Equations 1, 5, 9 and 10, predicts that the rate of reaction during an isothermal polymerization approaches zero when $\alpha = \alpha_m$. This condition represents the effect on the kinetic behaviour of a dramatic decrease of the molecular mobility due to the transition to a glassy state.

The values of the kinetic parameters of the model, evaluated by regression analysis, are listed in Table II. A comparison between the experimental DSC data and the model (Equations 1, 5, 9 and 10) predictions in isothermal conditions is reported in Figs 5 and 6.

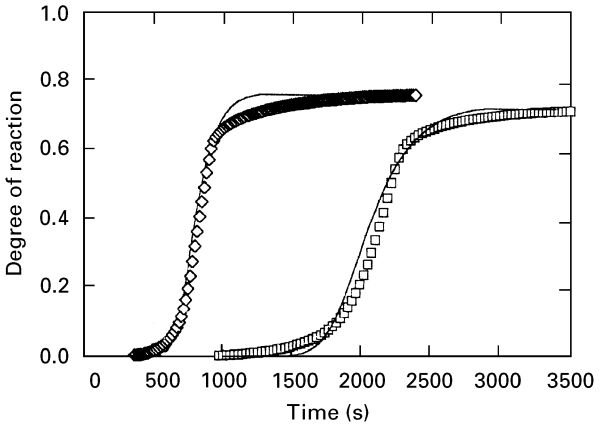

Figure 5 Comparison between kinetic model predictions and experimental degree of reaction data in isothermal conditions: □ 10 °C; ◇ 20 °C.

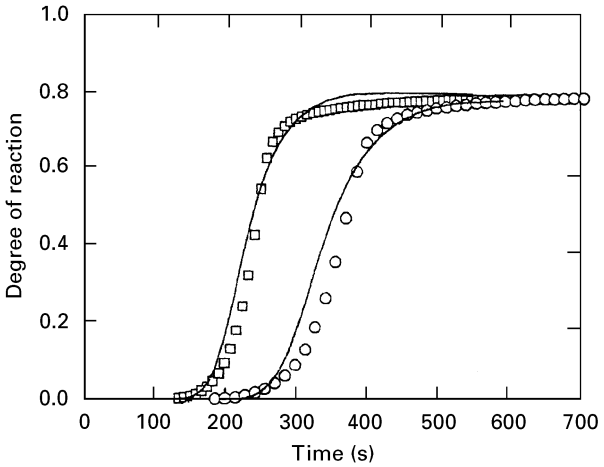

Figure 6 Comparison between kinetic model predictions and experimental degree of reaction data in isothermal conditions: ○ 30 °C; □ 35 °C.

In order to verify the model in non-isothermal conditions, a non-isothermal induction time, t_{ni}, calculated as the sum of the contributions at each isothermal temperature step must be introduced:

$$Q = \int_0^{t_{ni}} \frac{dt}{t_i} \tag{11}$$

where t_i is the isothermal induction time given by Equation 1 and Q is a dimensionless parameter ranging from 0 to 1. Numerical integration of Equation 11 is performed taking $t = 0$ at the initial temperature of the DSC experiment. The value $t = t_{ni}$ at which $Q = 1$, represents the non-isothermal induction time. Equation 11, representing the reaction between inhibitor and initiator for every thermal condition, must be integrated before propagation reaction starts (Equation 9). The comparison between experimental data and model predictions in non-isothermal conditions is shown in Fig. 7. The good agreement observed in Figs 5–7 indicates that a simple model can be used to represent the complex kinetic behaviour.

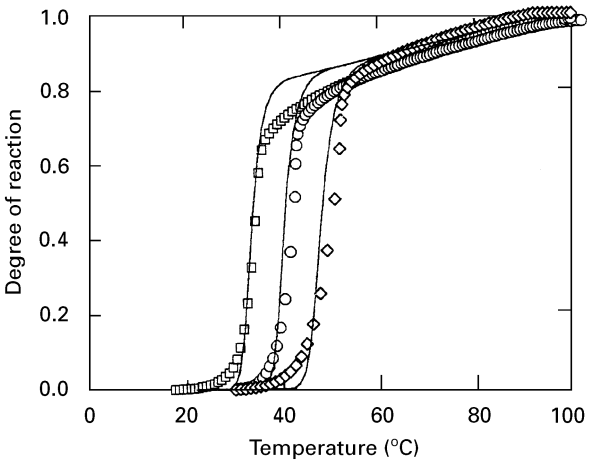

Figure 7 Comparison between kinetic model predictions and experimental degree of reaction data in non-isothermal conditions: □ 3 °C/min; 0.5 °C/min; ◇ 10 °C/min.

4. Simulation of *in situ* polymerization

4.1. Energy balance

During polymerization, heat is generated in the material due to the exothermic nature of the reaction. The rates of reaction are usually very high at typical polymerization temperatures and not all the heat can be dissipated fast enough to maintain isothermal conditions. The temperature inside the bone–cement–prosthesis system can be calculated by solving an energy balance coupled with an appropriate expression for the polymerization kinetics [9, 10].

Simulation of the non-isothermal polymerization behaviour of the studied bone cement during hip replacement procedures, is performed introducing the following assumptions:

1. Heat is dissipated only in the radial direction (r axis) according to the axial section sketched in Fig. 8.
2. The value of density, ρ, specific heat, C_p, and thermal conductivity, k_r, are taken as the literature values for bone [18], cement [10, 13] and a steel prosthesis [19], and are reported in Table III.

With these assumptions the law of conservation of energy in the bone and the prosthesis takes the form:

$$\rho_i C_{pi} \partial T/\partial t = k_{ri}(\partial^2 T/\partial r^2 + (1/r)\partial T/\partial r) \qquad i = b, p \tag{12}$$

indicating the properties of bone and prosthesis with the subscripts b and p, respectively. The energy balance in the cement must take into account the rate of heat generated by the chemical reactions (dQ/dt):

$$\rho_b C_{pc} \partial T/\partial t = k_{rc}(\partial^2 T/\partial r^2 + (1/r)\partial T/\partial r) + \rho_c \, dQ/dt \tag{13}$$

dQ/dt is given by Equation 4 but in this case the rate of reaction $d\alpha/dt$ is calculated from the kinetic model (Equations 5 and 9–11). Dimensionless numbers may be introduced in order to better understand the relative weight of the different terms of Equations 12 and 13 and to facilitate the numerical solution [8, 20]. The

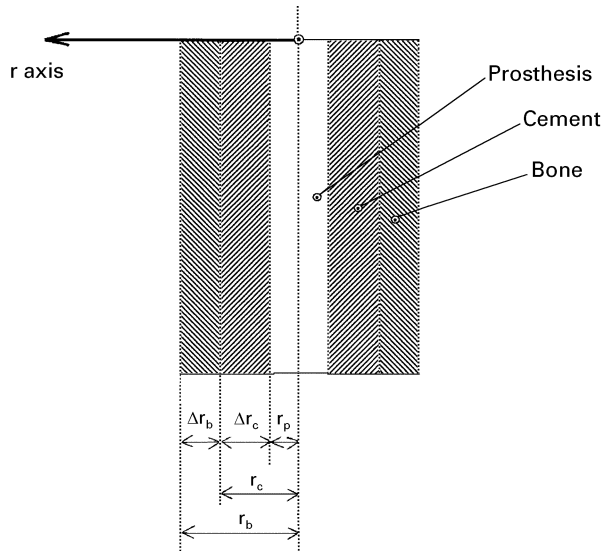

Figure 8 Sketch of the geometry used for the simulation of *in situ* polymerization of the bone cement.

dimensionless variables of the model are defined as:

$$\begin{aligned} &\text{dimensionless temperature} && \theta = (T - T_o)/(T_{ref} - T_o) \\ &\text{dimensionless time} && t^* = t/t_{1/2} \\ &\text{dimensionless position} && r^* = r/\Delta r_i \qquad i = p, c, b \end{aligned} \tag{14}$$

where Δr_i represents the radius of the prosthesis or the thickness of the cement or the bone (Fig. 8), T_o is the initial temperature of the cement, $T_{ref} = 37\,^{\circ}C$ is taken as reference temperature for evident reasons, and $t_{1/2}$ is defined as the time needed to reach a value of $\alpha = 0.5$. $t_{1/2}$ is obtained by numerical integration of the kinetic model given by Equations 5 and 9–11 at $T = T_{ref}$.

etic constant given by:

$$K^* = t_{1/2} K_o \tag{18}$$

In Equations 15 and 16, De_i is a dimensionless diffusion Deborah number [8, 20]:

$$De_i = k_{ri} t_{1/2}/\rho_i C_{pi} \Delta r_i \qquad i = b, p, c \tag{19}$$

The Deborah number represents the relationship between the heat transferred by conduction and the accumulation of heat in the material. Furthermore, in Equation 16 the Stefan number, St, is introduced:

$$St = Q_{tot}/[(T_{ref} - T_o)C_{pc}] \tag{20}$$

St may be considered as the relationship between the latent heat associated with the chemical reaction and the accumulation of heat in the material. Isothermal polymerization conditions are verified if, in the energy balance, the contribution of the thermal diffusivity (measured by the Deborah number) is much higher than the contribution of heat generation due to the polymerization reaction (measured by the Stefan number). On the other hand, adiabatic conditions are approached if De is one order of magnitude lower than 1. The Deborah numbers of the bone, of the prosthesis and of the cements are a measure of their ability to dissipate the heat generated in the cement by polymerization. For a given material characterized by constant values of t_g, k_x, ρ and C_p, the value of De is determined by its thickness.

In Equations 15–17 the initial conditions are:

$$\begin{aligned} &\text{prosthesis:} && t^* = 0 && \theta = \theta_{po} \\ &\text{cement:} && t^* = 0 && \theta = \theta_{co} \qquad \alpha = 0 \\ &\text{bone:} && t^* = 0 && \theta = 1 \end{aligned} \tag{21}$$

where θ_{po} and θ_{co} are given by Equation 14 calculated at the initial temperature of the prosthesis and cement, respectively. The dimensionless boundary conditions are:

$$\text{prosthesis:} \quad r^* = 0 \qquad \partial\theta/\partial r^* = 0 \tag{22}$$

$$r^* = 1 \qquad (\partial\theta/\partial r^*)_{r_p} = K^*_{rpc}(\partial\theta/\partial r^*)_{r_c}\,\theta_p(1) = \theta_c(0) \tag{23}$$

$$\text{cement:} \quad r^* = 0 \qquad (\partial\theta/\partial r^*)_{r_p} = K^*_{rpc}(\partial\theta/\partial r^*)_{r_c}\,\theta_p(1) = \theta_c(0) \tag{24}$$

$$r^* = 1 \qquad (\partial\theta/\partial r^*)_{r_c} = K^*_{rcb}(\partial\theta/\partial r^*)_{r_b}\,\theta_c(1) = \theta_b(0) \tag{25}$$

$$\text{bone:} \quad r^* = 0 \qquad (\partial\theta/\partial r^*)_{r_c} = K^*_{rcb}(\partial\theta/\partial r^*)_{r_b}\,\theta_p(1) = \theta_c(0) \tag{26}$$

$$r^* = 1 \qquad \theta = 1 \tag{27}$$

The final equations then become for the bone and the prosthesis:

$$\partial\theta/\partial t = De_i(\partial^2\theta/\partial r^{*2} + (1/r^*)\partial T/\partial r^*) \qquad i = b, p \tag{15}$$

and for the cement:

$$\partial\theta/\partial t = De_c(\partial^2\theta/\partial r^{*2} + (1/r^*)\partial T/\partial r^*) + St_c\,d\alpha/dt^* \tag{16}$$

$$d\alpha/dt^* = K^* \exp(-E_a/RT)\alpha^m(1-\alpha)\,(\alpha_m - \alpha)^n \tag{17}$$

Equation 17 is the dimensionless form of the kinetic model (Equation 9) where K^* is a dimensionless kin-

Equations 23–27 state that the equivalence of the heat flow and of the temperatures at the interface between prosthesis and cement and between cement and bone is imposed. The dimensionless groups

TABLE III Properties of bone, prosthesis and cement

Parameter	Prosthesis	Cement	Bone
k_r(W/mK)	10.3	0.17	0.43
C_p(J/gK)	0.5	1.7	1.25
ρ(g/cm^3)	7.8	1.1	1.7
Q_{tot}(J/g)		125	

K^*_{rpc} and K^*_{rcb} are defined as:

$$K^*_{rpc} = (k_c r_p)/(k_p r_c) \quad (28)$$

$$K^*_{rcb} = (k_b r_c)/(k_c r_b) \quad (29)$$

A numerical solution of the mathematical model presented (Equations 15–17) is performed using implicit finite differences.

4.2. Model results

Simulation of the polymerization process is performed according to the geometry sketched in Fig. 8. The thickness of the parts and the initial and boundary conditions are listed in Tables IV and V. In the proposed case studies, the effect of the cement thickness and of the insertion temperature are considered.

For simulations A and B (Table V) a preparation time of 4.3 min at 18 °C is assumed, in accordance with the data collected by Noble [10] from 21 total hip replacement procedures. The temperature and the degree of reaction as a function of time at the bone/cement interface, are reported in Figs 9 and 10 (simulations 1A, 2A and 3A). The Deborah numbers of the bone ($De_b = 0.29$) and of the cement, listed in Table VI, are one order of magnitude lower than the Stefan number for cement thickness of 5 and 7 mm, indicating that adiabatic conditions are approached. As shown in Fig. 10, the reaction simultaneously starts in every point across the cement thickness, determining a peak temperature at the bone/cement interface of about 50 °C and, inside the thicker cement layers, higher than 120 °C. The 3 mm thick cement layer presents a much lower peak temperature inside the cement, as shown in Table VI, but at the bone/cement interface the maximum temperature is very close (1 °C lower) to that calculated for the thicker layers. As reported by Brauer *et al.* [14], the threshold level for thermal tissue damage ranges from 48 °C to 60 °C, depending on the exposure time. At 50 °C, cell necrosis occurs with exposure between 30 s and 400 s. The exposure times at a temperature higher than 50 °C, calculated from the different simulations, are reported in Table VI. As shown in Fig. 9 and Table VI, the effect of a thicker cement layer is reflected in a longer exposure time at high temperature rather than in a higher peak temperature.

TABLE IV Radial dimensions of prosthesis, bone and cement adopted for simulations of the *in situ* polymerization process

Simulation number	Prosthesis radius (mm)	Cement thickness (mm)	Bone thickness (mm)
1A, 1B, 1C	10	3	8
2A, 2B, 2C	8	5	8
3A, 3B, 3C	6	7	8

TABLE V Initial and boundary conditions adopted for simulations of the *in situ* polymerization process

Simulation number	Prosthesis temp. (°C)	Cement temp. (°C)	Bone temp. (°C)
1A, 2A, 3A	18	18	37
1B, 2B, 3B	18	5	37
1C, 2C, 3C	18	30	37

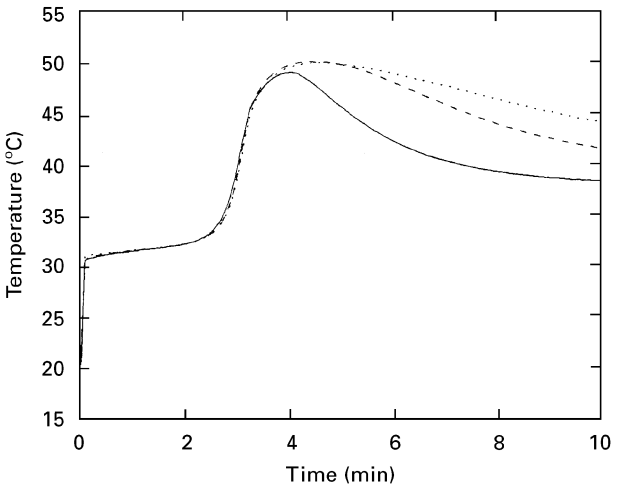

Figure 9 Results of the numerical simulation: temperature versus polymerization time at the bone/cement interface for three different thicknesses (simulations 1A, 2A, 3A): — 3 mm; – – – 5 mm,..... 7 mm.

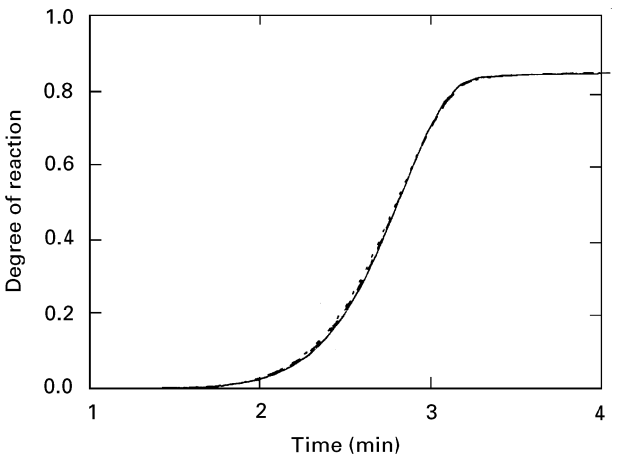

Figure 10 Results of the numerical simulation: degree of reaction versus polymerization time at the bone/cement interface for three different thicknesses (simulations 1A, 2A, 3A) : —— 3 mm; — — — 5 mm; – – – – – 7 mm.

TABLE VI Results of the simulations

Simulation number	PTC (°C)	PTBCI (°C)	T150 (s)	De_c	St
1A	97.8	49.0	0	0.77	3.9
2A	121.4	50.1	72	0.28	3.9
3A	123.7	50.1	84	0.14	3.9
1B	85.2	47.5	0	0.77	2.3
2B	120.7	48.1	0	0.28	2.3
3B	123.7	47.2	0	0.14	2.3
1C	102.3	52.0	70	0.77	3.9
2C	116.6	54.4	158	0.28	3.9
3C	116.7	54.4	213	0.14	3.9

PTC = maximum peak of temperature in the cement.
PTBCI = maximum peak of temperature at the bone/cement interface.
TI50 = exposure time to a temperature higher than 50 °C.

Fig. 10 indicates that unreacted monomer at the bone cement interface is still present in the cement at the end of polymerization. As a consequence of vitrification, the maximum temperature reached in the cement represents the limiting constraint for the maximum degree of reaction. So, if a temperature increase is detrimental for the tissues, it is beneficial for the maximum value of the degree of reaction that can be attained in the cement. If the temperature does not approach the onset of T_{gmax} (about 97 °C for the studied cement), the degree of reaction will remain lower than one and the unreacted monomer will be released at a rate dependent on its concentration in the cement and on the diffusion coefficient of MMA in the glassy cement. Analysis with dimensionless numbers suggests that isothermal polymerization can be achieved using a cement thickness of less than 0.5 mm. This value, too low to be used in surgical practice, corresponds to a value of $De = 27.7$, one order of magnitude higher than the Stefan number.

The results reported in Figs 11 and 12 are obtained when setting the cement temperature at 5 °C during the mixing and insertion time (simulations 1B, 2B, and 3B). In this case, if the *De* and *St* numbers are not significantly changed (Table VI), a lower temperature is calculated at the bone/cement interface. This result can be explained by considering that the heat is released in 2 min (Fig. 12), while in the former case

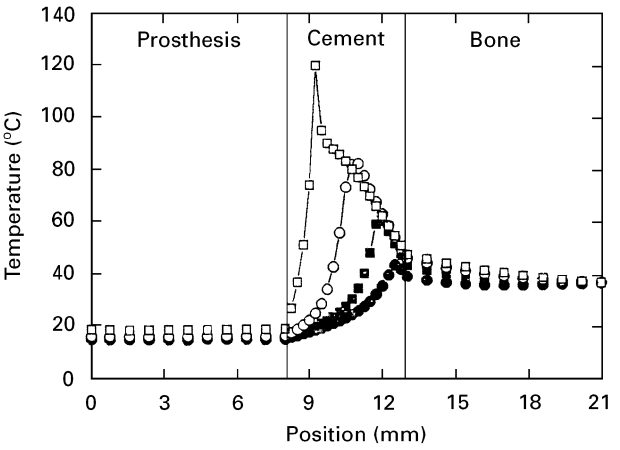

Figure 13 Temperature profiles across the prosthesis, cement and bone resulting from the numerical simulation, at different time intervals (simulation 2B): ● 5.2 min; ■ 5.7 min; ○ 6.2 min; □ 6.7 min.

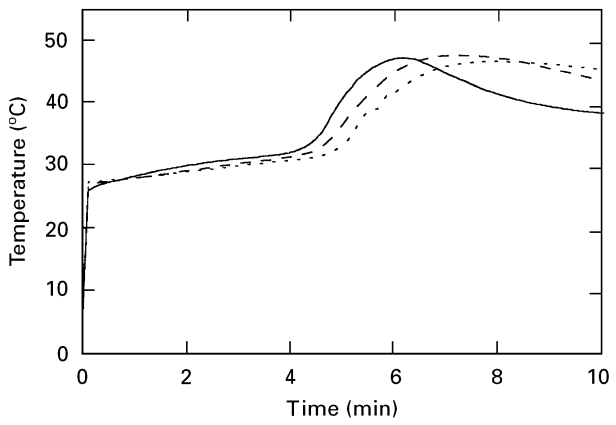

Figure 11 Results of the numerical simulation: temperature versus polymerization time at the bone/cement interface for three different thicknesses (simulations 1B, 2B, 3B): —— 3 mm; ——— 5 mm; – – – – – 7 mm.

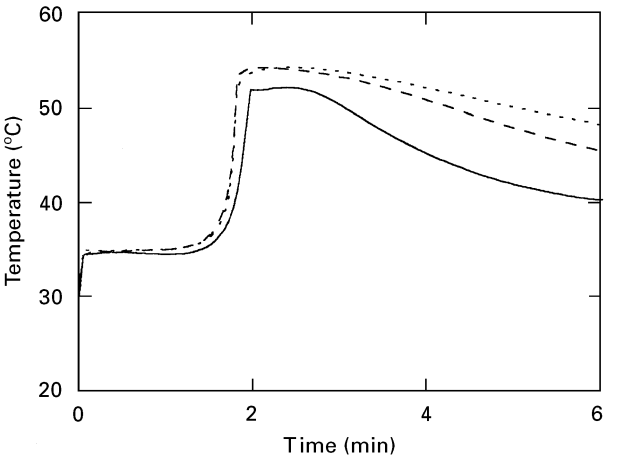

Figure 14 Results of the numerical simulation: temperature versus polymerization time at the bone/cement interface for three different thicknesses (simulations 1C, 2C, 3C): —— 3 mm; – – 5 mm; - - - - 7 mm.

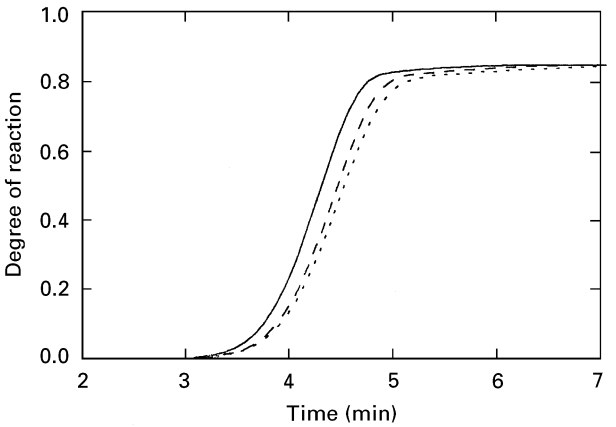

Figure 12 Results of the numerical simulation: degree of reaction versus polymerization time at the bone/cement interface for three different thicknesses (simulations 1B, 2B, 3B): — 3 mm; – – – 5 mm; - - - - 7 mm.

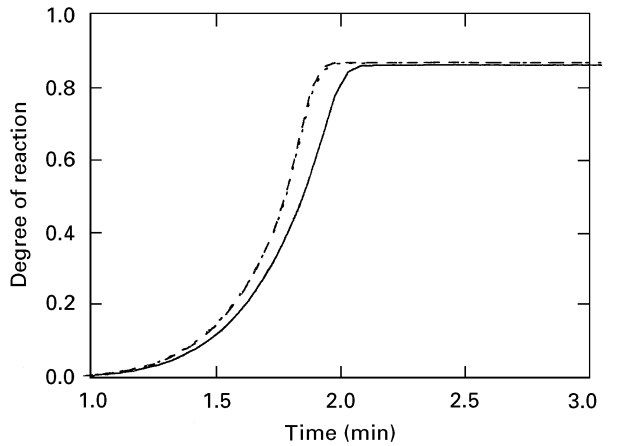

Figure 15 Results of the numerical simulation: degree of reaction versus polymerization time at the bone/cement interface for three different thicknesses (simulations 1C, 2C, 3C): — 3 mm; – – – 5 mm; - - - - - 7 mm.

(Fig. 10) it is released in 1.5 min. This effect is simply obtained by lowering the cement initial temperature. In this way, the steeper temperature gradient induced is responsible for a corresponding significant gradient of induction time that delays the onset of the reaction across the cement thickness. As shown in Fig. 13, where the temperature profiles across the thickness at different times are reported for the simulation 2B, a thermal wave propagates across the cement starting from the bone/cement interface. Once the reaction is started, the gel effect is responsible for the fast and uncontrolled heat generation.

The results reported in Figs 14 and 15 are obtained by considering a mixing phase of 1.5 min at 18 °C and a subsequent handling time of 1 min, that brings the cement in the bone cavity to a temperature of 30 °C (simulations 1C, 2C and 3C). Although the induction time is simultaneously consumed across the cement as in the case of Figs 9 and 10, the reaction starts when the average cement temperature is higher, determining a higher rate of reaction. In this case, as shown in Fig. 15, the heat is released in about 1 min and a maximum value of temperature of about 55 °C is calculated at the bone/cement interface, for the thicker layers. It must be noted that the high temperature reached inside the cement (Table VI) leads to a final degree of reaction $\alpha = 1$. For this reason the average value of α at the end of polymerization is higher than that shown in Figs 10, 12 and 15.

In summary, an increase of cement thickness affects the exposure time at the highest temperature rather than the maximum value of temperature at the bone/cement interface. According to the polymerization mechanism reported above (Equation 5 and Fig. 3), minimizing the peak temperature and maximizing the degree of reaction are two objectives that cannot be achieved simultaneously. However, the slope of the straight line shown in Fig. 3 is very low and therefore the change of 10 °C observed between the peak temperatures reported in Figs 11 and 14 is responsible for a moderate decrease, about 0.04, in the final degree of reaction, as shown in Figs 12 and 15. This last consideration suggests that the advantage of a temperature reduction may overcome the disadvantage of a higher content of unreacted MMA.

5. Conclusions

In this study, the isothermal and non-isothermal polymerization behaviour of a commercial bone cement has been described. A kinetic model accounting for the effects of induction time, autoacceleration and vitrification has been presented. This original model has been integrated with an energy balance in order to predict the temperature and the degree of reaction during the simulation of *in situ* polymerization of bone cement. The correct representation of polymerization kinetics is a key point for the calculation of temperature and degree of reaction profiles in order to properly take into account the heating rate generated by the polymerization reaction. The model has been applied to the study of the effects of different thicknesses and initial temperatures of the cement on temperature and degree of reaction profiles across the bone, cement and prosthesis.

It has been demonstrated that a low temperature and a high degree of reaction cannot be obtained simultaneously as a consequence of the diffusion effects dominating the polymerization reaction. Furthermore, wide differences of temperature have been calculated between the bone/cement interface and the central part of the cement. Reduction of the temperature at the bone/cement interface has been observed by reducing the cement temperature during mixing insertion operations.

References

1. G. ODIAN, "Principles of polymerization" (McGraw-Hill, New York, 1991).
2. J. M. DIONISIO and K. F. O'DRISCOLL, *J. Polym. Sci. Polym. Chem.* **18** (1980) 241.
3. H. K. MAHABADI and K. F. O'DRISCOLL, *Macromolecules* **10** (1977) 55.
4. I. MITA and K. HORIE, *JMS-Rev. Macromol. Chem. Phys.* **C27** (1987) 91.
5. R. SACK, G. V. SCHULZ and G. MEYERHOFF, *Macromolecules* **21** (1988) 3345.
6. S. T. BALKE and A. E. HAMIELEC, *J. Appl. Polym. Sci.* **17** (1973) 905.
7. K. A. HIGH, H. B. LEE and D. T. TURNER, *Macromolecules* **12** (1979) 332.
8. J. M. KENNY, A. MAFFEZZOLI and L. NICOLAIS, *Compos. Sci. Technol.* **38** (1990) 339.
9. A. MAFFEZZOLI, A. DELLA PIETRA, S. RENGO, L. NICOLAIS and G. VALLETTA, *Biomaterials* **15** (1994) 1221.
10. J. M. KENNY and A. TRIVISANO, *Polym. Engng. Sci.* **31** (1991) 1426.
11. P. C. NOBLE, *Biomaterials* **4** (1983) 94.
12. K. J. BUNDY and R. W. PENN, *J. Biomed. Mater. Res.* **21** (1987) 773.
13. S. SAHA and S. PAL, *ibid.* **18** (1984) 435.
14. G. M. BRAUER, D. R. STEINBERGER and J. W. STANSBURY, *ibid.* **20** (1986) 839.
15. A. MAFFEZZOLI and R. TERZI, *Thermochimica Acta.* **269–270** (1996) 319.
16. L. A. UTRACKI, "Polymer alloys and blends" (Hanser Verlag, Munich, 1990).
17. J. BRANDRUP and E. H. IMMERGUT, "Polymer handbook" (Wiley Interscience, New York, 1989).
18. D. G. FLEMING and B. N. FEINBERG, "Handbook of engineering in medicine and biology" (CRC Press, Cleveland, OH, 1978).
19. F. KREITH, "Principles of heat transfer" (Dun-Donnelley, New York, 1973).
20. A. MAFFEZZOLI, R. TERZI and L. NICOLAIS, *J. Mater. Sci. Mater. Med.* **6** (1995) 161.

Received 22 May 1995
and accepted 10 January 1996